Quantitative Determination of the Speciation of Surface Vanadium Oxides and Their Catalytic Activity

Hanjing Tian, Elizabeth I. Ross, and Israel E. Wachs*

Operando Molecular Spectroscopy and Catalysis Laboratory, Department of Chemical Engineering, 111 Research Drive, Iacocca Hall, Lehigh University, Bethlehem, Pennsylvania 18015

Received: October 10, 2005; In Final Form: March 24, 2006

A quantitative method based on UV−vis diffuse reflectance spectroscopy (DRS) was developed that allows determination of the fraction of monomeric and polymeric VO_x species that are present in vanadate materials. This new quantitative method allows determination of the distribution of monomeric and polymeric surface VO_x species present in dehydrated supported V_2O_5/SiO_2, V_2O_5/Al_2O_3, and V_2O_5/ZrO_2 catalysts below monolayer surface coverage when V_2O_5 nanoparticles are not present. Isolated surface VO_x species are exclusively present at low surface vanadia coverage on all the dehydrated oxide supports. However, polymeric surface VO_x species are also present on the dehydrated Al_2O_3 and ZrO_2 supports at intermediate surface coverage and the polymeric chains are the dominant surface vanadia species at monolayer surface coverage. The propane oxidative dehydrogenation (ODH) turnover frequency (TOF) values are essentially indistinguishable for the isolated and polymeric surface VO_x species on the same oxide support, and are also not affected by the Brønsted acidity or reducibility of the surface VO_x species. The propane ODH TOF, however, varies by more than an order of magnitude with the specific oxide support ($ZrO_2 > Al_2O_3 \gg SiO_2$) for both the isolated and polymeric surface VO_x species. These new findings reveal that the support cation is a potent ligand that directly influences the reactivity of the bridging V−O−support bond, the catalytic active site, by controlling its basic character with the support electronegativity. These new fundamental insights about polymerization extent of surface vanadia species on SiO_2, Al_2O_3, and ZrO_2 are also applicable to other supported vanadia catalysts (e.g., CeO_2, TiO_2, Nb_2O_5) as well as other supported metal oxide (e.g., CrO_3, MoO_3, WO_3) catalyst systems.

1. Introduction

Supported vanadia catalysts constitute a very important class of catalytic materials because they have become the model catalytic systems for fundamental studies of supported metal oxides and are extensively employed as commercial catalysts (oxidation of *o*-xylene to phthalic anhydride, selective catalytic reduction (SCR) of NO_x with NH_3 to N_2 and H_2O, oxidative destruction of chlorinated hydrocarbons, and ammoxidation of alkyl aromatics to aromatic nitriles).[1−3] In recent years, supported vanadia catalysts have also received much attention for selective oxidation and ammoxidation of C_1-C_4 hydrocarbons to olefins, oxygenates, and nitriles.[4−10]

The molecular structures of the supported vanadia phase on oxide supports have been extensively characterized by different spectroscopic techniques (IR, Raman, XANES/EXAFS, UV−vis diffuse reflectance spectroscopy (DRS), solid-state ^{51}V NMR, etc.).[11−28] Under dehydrated conditions, four different types of vanadia species have been identified in supported vanadia catalysts: (1) isolated surface VO_4 species containing one terminal V═O bond and three bridging V−O−support bonds, (2) polymeric surface VO_4 species containing one terminal V═O bond and three bridging V−O−V/V−O−support bonds, (3) crystalline V_2O_5 nanoparticles (NPs), and (4) mixed oxide compounds or solid solutions with some oxide supports at elevated temperatures (e.g., $Zr(V_2O_7)_2$, $AlVO_4$, $V_xTi_{1-x}O_2$, $NbVO_5$, $Mg_3(VO_4)_2$, $Mg_2V_2O_7$). Dehydrated surface VO_5/VO_6 species, if present at all, must constitute a very small fraction of the dehydrated surface vanadia species since their presence in spectroscopically detectable amounts has not been established. Minor amounts of V_2O_5 NPs with distorted VO_5 coordination, however, can also be present in catalysts with incompletely dispersed vanadia below monolayer surface coverage[28] and should not be confused with the surface VO_x species. In such cases, the spontaneous dispersion of V_2O_5 NPs onto the exposed support sites as surface vanadia species can occur by heating to elevated temperatures.[28,29] Below monolayer surface coverage (~8 V/nm^2), isolated monomeric and polymeric surface VO_4 species are the dominant surface vanadia species and V_2O_5 NPs only become significant above monolayer surface coverage when the available support surface sites become saturated with the surface vanadia species.

Catalytic studies for many different oxidation reactions have demonstrated that the monomeric and polymeric surface VO_4 species are generally the catalytic active sites in supported vanadia catalysts since the crystalline phases possess very few exposed active surface sites or low turnover frequencies (TOFs; TOF is the number of molecules converted per catalytic active site per second and is a quantitative measure of the efficiency per exposed catalytic active site).[4−9,19,20,22,27,30−33] The individual catalytic contributions of the isolated VO_4 and polymeric VO_4 species during these catalytic reactions, however, are still not completely resolved in the literature.

Determination of the individual catalytic contributions of isolated and polymeric surface vanadia species on oxide supports requires that these vanadia species be quantified under dehydrated conditions. Schoonheydt et al. have shown that the UV−

* Corresponding author. Telephone: (610) 758-4274. Fax: (610) 758-6555. E-mail: iew0@lehigh.edu.

10.1021/jp055767y CCC: $33.50
Published on Web 04/21/2006

vis DRS signal can quantify both the V^{5+} and V^{4+} species below 1% V on alumina and other catalyst support materials.[24] The V^{5+} UV−vis DRS signal was monitored with the ligand to metal charge transfer (LMCT) transition, and the V^{4+} UV−vis DRS signal was monitored with the d−d transition. Complementary quantitative ESR spectroscopy was also employed to confirm the V^{4+} UV−vis DRS quantitative measurements of the catalysts, and both techniques were in excellent agreement. Argyle et al. quantified the extent of reduction of surface vanadia on alumina by monitoring the changes in the V^{4+} d−d transition and titrating the reduced V^{4+} species with molecular O_2 to V^{5+}.[27] Neither of these investigations, however, attempted to quantify the amount of isolated and polymeric surface V^{5+} species on oxide supports below monolayer surface coverage. During typical propane oxidative dehydrogenation (ODH) reaction conditions, the surface vanadia species are almost completely present as surface V^{5+} species because of the relatively weak reducing power of propane and the excess of molecular O_2 that is typically employed.[5,20,22,27]

In the present investigation, UV−vis DRS is employed to quantify the concentration of monomeric and polymeric surface vanadia species because this spectroscopic method exhibits unique electronic transitions for different vanadia structures (isolated vs polymeric structures).[24] The V^{5+} LMCT transition shifts to lower energy values with extent of vanadia polymerization as a consequence of greater electron delocalization in polymerized structures.[20−27] This has led some authors to employ the UV−vis edge energy (E_g) value as a parameter to qualitatively monitor the extent of vanadia polymerization.[19−22,27,30,31] This approach is related to the quantum confinement effect of small domains since the E_g value monotonically decreases with the number of bridging V−O−V bonds in the vanadia structure (E_g: $V^0 > V^1 > V^2 > V^3 > V^4 > V^5 > V^6$, where the superscript represents the number of bridging V−O−V bonds in the VO_x unit).[21] The quantitative UV−vis DRS method is developed and applied to determine the relative surface concentrations of the monomeric and polymeric surface VO_4 species that are present in dehydrated supported vanadia catalysts (V_2O_5/SiO_2, V_2O_5/Al_2O_3, and V_2O_5/ZrO_2). This quantitative information is subsequently used to develop the molecular structure−activity relationship for propane oxidative dehydrogenation (ODH) to propylene over the supported vanadia catalysts.

2. Experimental Section

Catalyst Synthesis. The oxide supports used for this study were SiO_2 (Cabot, Cab-O-Sil EH-5, $S_{BET} = 330$ m^2/g), Al_2O_3 (Engelhard, $S_{BET} = 222$ m^2/g), and ZrO_2 (Degussa, $S_{BET} = 39$ m^2/g). The supported vanadia catalysts were prepared by the incipient wetness impregnation of 2-propanol solutions of vanadium isopropoxide ($VO(O-Pr^i)_3$, Alfa-Aesar, 97% purity). Impregnation was performed inside a glovebox with continuously flowing N_2, and the samples were dried overnight at room temperature in the flowing N_2 environment. The samples were further dried in flowing N_2 at 120 °C for 1 h and 300 °C for another 1 h, and subsequently calcined in flowing air at 300 °C for 1 h and 450 °C for another 2 h to form the supported vanadia catalysts.

Raman Spectroscopy. The *in situ* Raman spectra in this study were collected with a combined UV/visible Raman spectrometer system (Horiba-Jobin Yvon LabRam-HR) equipped with a confocal microscope (Olympus BX-30), notch filter (532 nm), and single stage monochromator (Horina-Jobin Yvon LabRam-HR), and a 900 grooves/mm grating. The Raman spectra in this study were collected with visible laser excitation at 532 nm (20 mW, YAG laser) in the 300−1100 cm^{-1} region. The laser power at the sample was kept below 0.5 mW to minimize any laser-induced alterations of the sample. The scattered photons passed through the notch filter and grating in the monochromator to remove the Rayleigh scattering, and were collected with a UV/visible sensitive LN_2-cooled CCD detector (Horiba-Jobin Yvon CCD-3000V). The spectral resolution of the Horiba-Jobin Yvon LabRam-HR is ∼1 cm^{-1} for the given parameters. The supported vanadia catalysts were loaded in powder form into an *in situ* cell (Linkam, TS1500) that allowed for sample treatments such as dehydration. The dehydrated Raman spectra were collected at room temperature in flowing 10% O_2/He (30 mL/min) after being dehydrated at 400 °C for 1 h in the flowing O_2/He to desorb the adsorbed moisture.

UV−Vis Diffuse Reflectance Spectroscopy. The *in situ* UV−vis DRS spectra were obtained with a Varian Cary 5E UV−vis spectrophotometer employing the integration sphere diffuse reflectance attachment. The finely ground powder samples of the bulk vanadate reference samples and the supported vanadia catalysts were loaded into an *in situ* cell (Harrick, HVC-DR2) and measured in the region of 200−800 nm at room temperature. A MgO reflectance standard was used as the baseline. The UV−vis DRS spectra of the bulk vanadate reference compounds were obtained under ambient conditions, and the spectra of the dehydrated supported vanadia catalysts were obtained after the samples were treated at 400 °C in flowing 10% O_2/He gas (30 mL/min) for 1 h to desorb the adsorbed ambient moisture. To minimize the effects of regular reflection and particle size, the samples were diluted with MgO. The amount of diluent used for a sample depended on the absorbance of the sample, which should result in the Kubelka−Munk function $F(R_\infty) < 1$ after dilution. The Kubelka−Munk function $F(R_\infty)$ was extracted from the UV−vis DRS absorbance and the edge energy (E_g) for allowed transitions was determined by finding the intercept of the straight line in the low-energy rise of the plot of $[F(R_\infty)h\nu]^2$against $h\nu$, where $h\nu$ is the incident photon energy.[21]

Propane ODH over Supported Vanadia Catalysts. Propane oxidative dehydrogenation was carried out in an isothermal fixed-bed differential reactor (Pyrex tubing, 1/4 in. outside diameter and 1 ft long) using 20−100 mg of catalyst at atmospheric pressure. The reactant gas mixtures consisted of 18% C_3H_8/6% O_2/He (total 100 mL/min). The reactor effluent was analyzed by an on-line gas chromatograph (Hewlett-Packard 6890 Series) equipped with both a thermal conductivity detector (Carboxene-1000 packed column) and a flame ionization detector (Supelco capillary column (PQ1334-04)). The samples were pretreated in flowing O_2/He at 450 °C for 0.5 h before each run. The catalytic activity values, as measured by turnover frequency (the number of propane molecules converted per V atom per second), were obtained at the reaction temperature of 300 °C. The propane conversions were kept below 3% to avoid secondary reactions and to minimize heat and mass transfer limitations.

3. Results

Raman Spectroscopy. It is critical to confirm the absence of V_2O_5 NPs in the supported vanadia catalysts since their presence can affect the quantitative UV−vis DRS measurements of the surface vanadia species. The UV−vis DRS transitions are generally quite broad, and the presence of V_2O_5 NPs, which have a low E_g value of 2.3 eV resulting from the five bridging V−O−V bonds in the structure, will shift the broad band toward

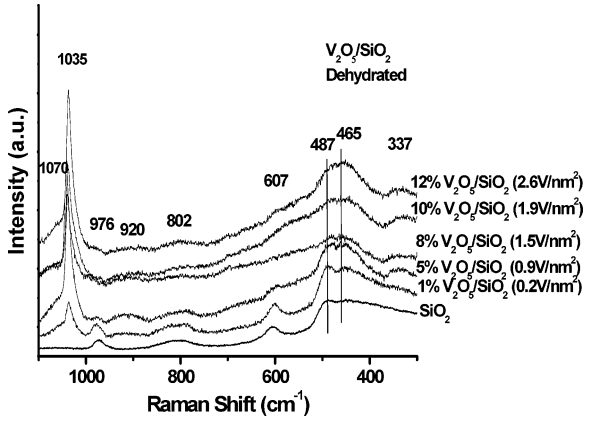

Figure 1. *In situ* Raman spectra of dehydrated supported V_2O_5/SiO_2 catalysts as a function of vanadia loading.

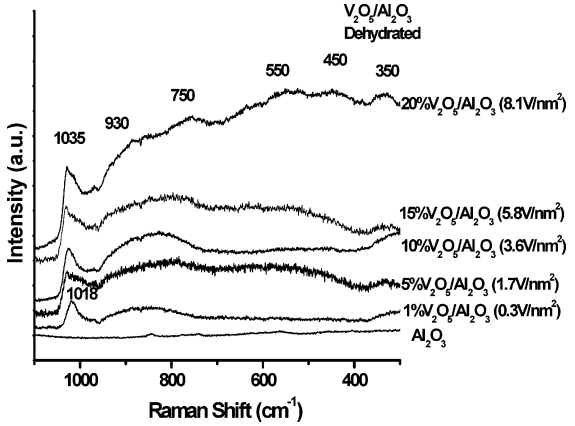

Figure 2. *In situ* Raman spectra of dehydrated supported V_2O_5/Al_2O_3 catalysts as function of vanadia loading.

the lower energy region and skew the quantitative results. Raman spectra, however, tend to give rise to sharp bands that allow discrimination between the different molecular structures. This is especially true for the detection of V_2O_5 NPs since their characteristic Raman bands, when excited in the visible range (514.5−532 nm), are typically about 10 times stronger than the two-dimensional surface vanadia species on oxide supports.[34] Thus, the quantitative determination of the two-dimensional isolated and polymeric surface vanadia species by UV−vis DRS requires that three-dimensional vanadia structures, crystalline V_2O_5 NPs and mixed metal vanadate NPs containing multiple bridging V−O−V bonds, not be present in the current samples being employed for quantification. In addition, the Raman spectrum also contains complementary information about the dehydration extent of the catalysts and the nature of isolated and polymeric surface vanadia species since the bridging V−O−V bond vibrational modes are Raman active.

The Raman spectra of the dehydrated supported V_2O_5/SiO_2 catalysts are presented in Figure 1 as a function of vanadia loading (0.2−2.6 V/nm^2). The SiO_2 support gives rise to Raman bands at 976, 802, 607, and 487 cm^{-1} originating from Si−OH vibrations (976 cm^{-1}) and three to five Si-containing siloxane rings (802, 607, and 487 cm^{-1}).[19] The addition of vanadia to SiO_2 results in the consumption of the surface Si−OH sites, as reflected in the decrease of the 976 cm^{-1} band, and the preferential anchoring of the surface VO_4 units on the three-member siloxane rings, revealed by the selective decrease of the 607 cm^{-1} band. The addition of vanadia to SiO_2 also produces several new Raman bands at 1070, 1035, 920, 465, and 337 cm^{-1}. The broad Raman bands at ∼1070 and ∼920 cm^{-1} have previously been assigned to Si−O bonds created by the breaking of Si−O−Si siloxane bonds during the anchoring of surface vanadia onto the silica support.[19] The broad ∼920 cm^{-1} band is also observed on other supported vanadia catalysts and may possibly originate from the vibration of the bridging V−O−silica bond.[16] The sharp Raman band present at ∼1035 cm^{-1} is associated with the fully dehydrated terminal monoxo V═O bond of surface VO_4 species bonded to the SiO_2 surface (O═V(−O−Si)$_3$) and essentially remains at the same position and increases in intensity with increasing surface vanadia coverage.[4,8,12,16,19,20] The Raman bands at 337 and 465 cm^{-1} originate from the ν_s and ν_{as} bending modes of the surface VO_4 species, respectively. Furthermore, the surface VO_4 species appear to be isolated since no Raman bands from bridging V−O−V bonds are detectable (see UV−vis section below for additional details). Above 12% V_2O_5/SiO_2, crystalline V_2O_5 NPs are also present on the silica support with a distinct and sharp Raman band at 994 cm^{-1} (not shown for brevity). Thus, the maximum dispersion of vanadia on this SiO_2 support as a surface VO_4 species corresponds to ∼12% V_2O_5/SiO_2 (∼2.6 V/nm^2) with the employed synthesis method. The low surface VO_4 density achievable on SiO_2 is well documented in the literature and is related to the low reactivity of the surface Si−OH groups relative to other oxide supports.[4,8,12,14,16,19,20,22,34]

The Raman spectra of the dehydrated supported V_2O_5/Al_2O_3 catalysts are shown in Figure 2 as a function of vanadia loading (0.3−8.1 V/nm^2). This high surface area transitional alumina support does not give rise to any Raman active bands, and consequently all the observed Raman bands originate from the supported vanadia phase. Further increase in vanadia content results in strong Raman bands due to the presence of crystalline V_2O_5 NPs (not shown for brevity), which indicates that monolayer surface vanadia coverage on this Al_2O_3 support corresponds to ∼20% V_2O_5/Al_2O_3 (8.1 V/nm^2). As the surface vanadia coverage increases in the submonolayer region, the strong Raman band above 1000 cm^{-1} broadens and shifts from 1018 to 1035 cm^{-1} and new broad bands appear at ∼930, ∼750, ∼550, ∼450, and ∼350 cm^{-1}. The Raman bands at 1018−1035 cm^{-1} originate from the symmetric vibration of the fully dehydrated terminal monoxo V═O bond of the surface VO_4 species.[8,14,17,20,27,31] The Raman bands at ∼550 and ∼750 cm^{-1} have previously been assigned to the ν_s and ν_{as} vibrational modes, respectively, of the bridging V−O−V bonds of the polymeric surface VO_4 species.[17,20] The Raman bands at ∼350 and 450 cm^{-1} originate from the ν_s and ν_{as} bending modes of the surface VO_4 unit, respectively. The broad band at ∼930 cm^{-1} has recently been assigned to the bridging V−O−alumina based on density functional theoretical (DFT) calculations.[16] The Raman spectra nicely reveal that crystalline V_2O_5 NPs are completely absent for these supported V_2O_5/Al_2O_3 catalysts below monolayer surface vanadia coverage and that the surface VO_4 species become polymerized with increasing surface vanadia coverage on the alumina support as demonstrated by the presence of bridging V−O−V vibrations.

The Raman spectra of the dehydrated supported V_2O_5/ZrO_2 catalysts are presented in Figure 3 as a function of vanadia loading (2.0−8.1 V/nm^2). The ZrO_2 support gives rise to the strong Raman bands at 630, 610, 552, 528, 480, 375, and 330 cm^{-1} that are associated with the ZrO_2 monoclinic phase. Unfortunately, these strong Raman bands from the ZrO_2 support prevent the collection of the vibrational modes of the surface vanadia species below 700 cm^{-1}. The addition of vanadia to the ZrO_2 support results in a new Raman band above 1000 cm^{-1} that shifts from 1027 to 1036 cm^{-1} with increasing surface

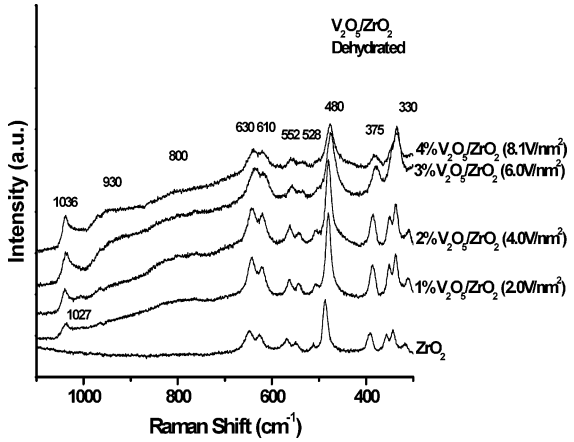

Figure 3. *In situ* Raman spectra of dehydrated supported V_2O_5/ZrO_2 catalysts as function of vanadia loading.

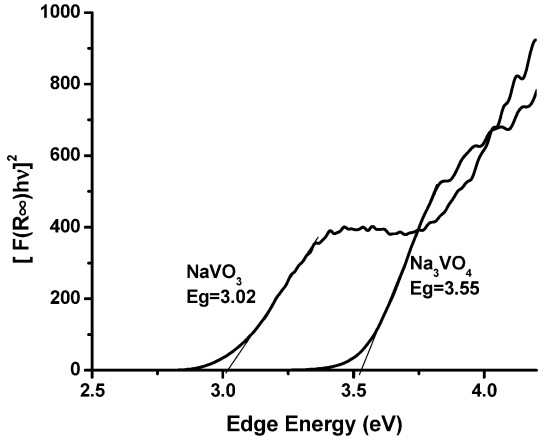

Figure 4. UV−vis DRS spectra and E_g values of bulk orthovanadate Na_3VO_4 (100% VO_4 coordinated monomer) and bulk metavandate $NaVO_3$ (100% VO_4 coordinated polymer).

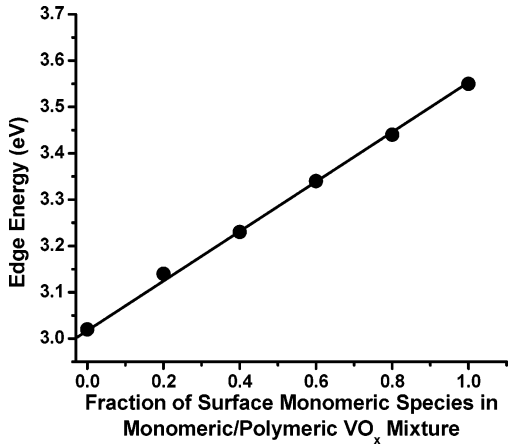

Figure 5. Correlation of vanadate E_g values with the fraction of isolated monomeric VO_4 units in samples containing physical mixtures of bulk Na_3VO_4 (100% VO_4 coordinated monomer) and $NaVO_3$ (100% VO_4 coordinated polymer)

vanadia density. This vibration is characteristic of the fully dehydrated terminal monoxo V═O bond of the surface VO_4 species.[8,20,22,30−32] Broad Raman bands are also observed at ~800 and 930 cm^{-1} associated with the ν_{as} vibration of bridging V−O−V bonds[1−3] and bridging V−O−zirconia bonds,[16] respectively. Crystalline V_2O_5 NPs are not present in any of the submonolayer (<8.1 V/nm^2) samples and only become significant above monolayer surface coverage (not shown for brevity). Thus, crystalline V_2O_5 NPs are not present in these catalysts and only surface monomeric and polymeric surface VO_4 species are present in the 1−4% V_2O_5/ZrO_2 supported catalysts, with the latter increasing in concentration with increasing surface vanadia coverage.

In summary, the Raman spectra revealed that for the supported vanadia catalysts and experimental conditions employed in the present investigation (1) crystalline V_2O_5 NPs are not present below monolayer surface coverage, (2) only two-dimensional surface vanadia species are present below monolayer surface coverage, (3) only isolated surface vanadia species are present at low surface coverage on the different oxide supports, (4) polymeric surface vanadia species are present at high surface coverage on Al_2O_3 and ZrO_2 supports, and (5) fully dehydrated surface vanadia species are obtained with the current dehydration pretreatments.

UV−vis Diffuse Reflectance Spectroscopy. It has been previously demonstrated that a linear relationship exists between the UV−vis DRS edge energy, E_g (eV), and the number of bridging V−O−V bonds present in bulk vanadate structures.[21] This general relationship has also been found to be independent of the local coordination for VO_x,[21] MoO_x,[35] and WO_x[36] reference compounds and only dependent on the number of bridging M−O−M bonds present in the structures. The number of bridging V−O−V bonds for VO_x coordinated vanadate materials varies from zero for isolated species to two for polymeric VO_4 chain species. The bulk orthovandate Na_3VO_4 and metavandate $NaVO_3$ compounds contain isolated VO_4 units and polymeric VO_4 chains,[37,38] respectively, that are analogous to the dehydrated surface VO_4 species present in supported vanadia catalysts. Thus it is possible to develop a quantitative relationship between the UV−vis edge energy and the number of bridging V−O−V bonds present in physical mixtures of bulk vanadates and to apply this relationship to the dehydrated surface VO_4 species. This assumes that the polymeric surface VO_4 species can be represented by polymeric VO_4 metavandate species. The UV−vis DRS spectra of bulk Na_3VO_4 (consisting of isolated VO_4 units) and bulk $NaVO_3$ (consisting of polymeric VO_4 chains) are shown in Figure 4. The E_g values for the bulk Na_3VO_4 and bulk $NaVO_3$ reference compounds are 3.55 and 3.02 eV, respectively. The corresponding E_g values for their physical mixtures are plotted vs the fraction of monomeric VO_4 units in the physical mixture in Figure 5. The intermediate E_g values for the physical mixtures vary linearly between the E_g values of bulk Na_3VO_4 and bulk $NaVO_3$, and can be represented by the linear equation

$$E_g = 3.02 + 0.53X_m \quad \text{(eV)} \qquad (1)$$

where X_m refers to the fraction of monomer in the sample.

The UV−vis DRS E_g values of the dehydrated supported V_2O_5/SiO_2, V_2O_5/Al_2O_3, and V_2O_5/ZrO_2 catalysts are tabulated in Table 1. Note that the E_g values for the dehydrated supported vanadia catalysts exactly span the same edge energy range (3.01−3.63 eV) shown above for the bulk vanadate VO_4-containing compounds (3.02−3.55 eV). The coincidence of the bulk and dehydrated supported vanadia catalysts strongly supports the conclusion in the literature that dehydrated surface vanadia species possess VO_4 coordination. Polymeric VO_5/VO_6 structures can possess more than two bridging V−O−V bonds and give rise to much lower E_g values (2.3−2.8 eV).[21] Hydration of the 20% V_2O_5/Al_2O_3 samples transforms the dehydrated surface VO_4 polymers to VO_6 coordinated $V_{10}O_{28}\cdot nH_2O$ clusters[1,2,21] containing five bridging V−O−V bonds and decreases the E_g value to 2.65 eV. The hydration results further confirm

TABLE 1: Edge Energy Values and Concentration of Surface Monomeric/Polymeric VO_4 Species for Dehydrated Supported Vanadia Catalysts

catalysts (dehydrated)	E_g (eV)	monomeric VO_x (%)	polymeric VO_x (%)
1% V_2O_5/Al_2O_3	3.63	100	0
3% V_2O_5/Al_2O_3	3.62	100	0
5% V_2O_5/Al_2O_3	3.50	90	10
10% V_2O_5/Al_2O_3	3.28	50	50
15% V_2O_5/Al_2O_3	3.10	16	84
20% V_2O_5/Al_2O_3	3.01	0	100
1% V_2O_5/SiO_2	3.55	100	0
5% V_2O_5/SiO_2	3.52	95	5
10% V_2O_5/SiO_2	3.52	95	5
12% V_2O_5/SiO_2	3.52	95	5
1% V_2O_5/ZrO_2	3.50	90	10
2% V_2O_5/ZrO_2	3.40	73	27
3% V_2O_5/ZrO_2	3.27	48	52
4% V_2O_5/ZrO_2	3.12	20	80

the absence of any significant concentration of surface VO_6 coordinated species for the dehydrated supported vanadia catalysts. The fractions of dehydrated polymeric surface VO_4 species present on the SiO_2, Al_2O_3, and ZrO_2 supports as a function of surface vanadia coverage were determined from the reference relationship established for the bulk vanadate compounds in Figure 5 and are presented in Table 1 and also plotted in Figure 6. The small amount of polymeric surface VO_4 species estimated on SiO_2 at intermediate coverage is within the UV−vis DRS experimental error. The general trend is that dehydrated isolated surface VO_4 species predominate at low surface coverage and the fraction of dehydrated polymeric surface VO_4 species increases with increasing surface coverage up to monolayer with the extent of polymerization following the trend $Al_2O_3 > ZrO_2 \gg SiO_2$ for the same surface vanadia density.

The analogous UV−vis DRS spectra for the dehydrated as well as hydrated supported vanadia catalysts have previously been reported.[19−22] Thus, only several representative UV−vis DRS spectra containing ∼100% monomer (1% V_2O_5/SiO_2), about 50% polymer/50% monomer (10% V_2O_5/Al_2O_3), and ∼100% polymer (20% V_2O_5/Al_2O_3) are presented in Figure 7 to show how the Kubelka−Munk function was utilized to determine the E_g values. The UV−vis DRS measurements were limited to these three oxide supports because of their weak absorption in the UV−vis region (200−800 nm range). Oxide supports possessing strong UV−vis DRS absorption (e.g., TiO_2, Nb_2O_5, CeO_2), unfortunately, overshadow the UV−vis DRS spectra of the surface vanadia species and prevent accurate determination of the E_g values for the surface vanadia species on these supports.[21]

In summary, the UV−vis spectra of dehydrated supported vanadia catalysts revealed that (1) the surface vanadia species can be accounted for by assuming only the presence of monomeric and polymeric dehydrated surface VO_4 species (as long as crystalline V_2O_5 nanoparticles are not present to skew the measurement to lower E_g values), (2) isolated surface VO_4 species predominate at low surface vanadia coverage, (3) both isolated and polymerized surface VO_4 species are present at intermediate surface coverage (with the exception of SiO_2 where isolated surface VO_4 species are almost exclusively present), and (4) polymeric surface VO_4 species predominate at high surface coverage (with the exception of SiO_2).

Propane ODH over Supported Vanadia Catalysts. The oxidative dehydrogenation of propane to propylene was also investigated over the supported vanadia catalysts to determine the relative contribution of isolated and polymeric surface VO_4 species for this catalytic reaction. The surface VO_4 species

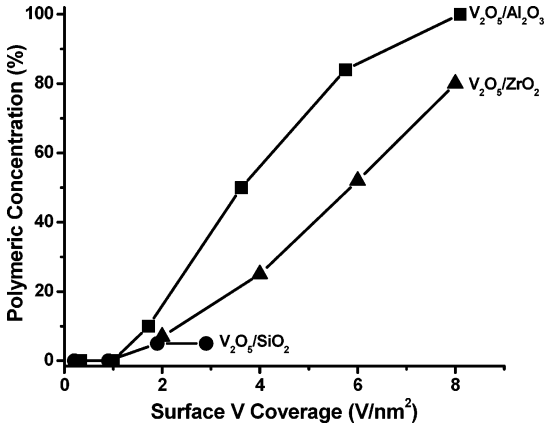

Figure 6. Fraction of surface polymeric VO_4 species for dehydrated supported vanadia catalysts as a function of surface vanadia coverage.

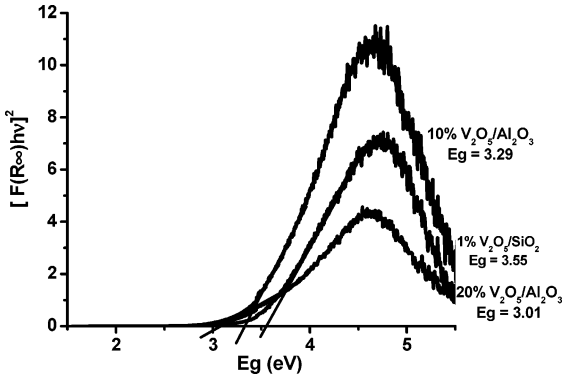

Figure 7. UV−vis DRS spectra and E_g values of dehydrated 20% V_2O_5/Al_2O_3, 1% V_2O_5/SiO_2, and 10% V_2O_5/Al_2O_3 catalysts.

remain both dehydrated and almost fully oxidized under the chosen propane ODH reaction conditions due to the high reaction temperatures (350−450 °C) and the low reactivity of propane coupled with the relatively rapid reoxidation of the reduced sites.[5,20,22,27] Consequently, essentially the same surface vanadia species are present under typical propane ODH reaction conditions as shown above for the dehydrated surface VO_4 species on the different supports. The influence of surface vanadia coverage on the TOF and selectivity values for propane ODH to propylene is given in Table 2 for the different supported vanadia catalysts. The propylene selectivity for supported V_2O_5/Al_2O_3 and V_2O_5/ZrO_2 catalysts systematically increases and the corresponding CO_2 selectivity slightly decreases with increasing surface vanadia coverage. These slight selectivity trends reflect the covering of the unselective exposed support sites by the surface vanadia species.[22] Figure 8 shows that the propane ODH TOF values over the supported vanadia catalysts are relatively constant for each support and are not affected by the extent of polymerization of the surface vanadia species. The TOF values, however, are strongly dependent on the specific oxide support: $ZrO_2 > Al_2O_3 > SiO_2$.

The number of surface VO_4 sites involved in the rate-determining step of propane ODH to propylene can also be determined from the simplified rate equation

$$r \quad (\text{mol/g·s}) = k' P_{C3} V^n \tag{2}$$

$$k' = k_{RDS} K_{ADS} \tag{3}$$

where V represents the number of vanadia atoms per gram of catalyst, k_{RDS} is the kinetic rate constant of the rate-determining step (rds), K_{ADS} is the propane equilibrium adsorption constant,

TABLE 2: TOF and Selectivity of Propane ODH to Propylene over Supported Vanadia Catalysts (350 °C, 18% C_3H_8/6% O_2/He, and Total Flow Rate of 100 mL/min)

				selectivity			
catalyst	surface coverage (V/nm^2)	A_c (mmol/g·h)	TOF (10^{-4} s^{-1})	C_3H_6	CO	CO_2	oxygenates
3% V_2O_5/Al_2O_3	1.0	15.5	13	67.0	11.5	21.5	
5% V_2O_5/Al_2O_3	1.7	23.7	12	69.3	10.2	20.5	
10% V_2O_5/Al_2O_3	3.6	51.4	13	75.6	8.8	15.6	
15% V_2O_5/Al_2O_3	5.8	59.3	10	80.8	10.9	7.2	1.1
20% V_2O_5/Al_2O_3	8.1	110.8	14	80.2	9.1	10.7	
5% V_2O_5/SiO_2	1.5	8.7	2.8	67.4	22.1	10.5	
10% V_2O_5/SiO_2	1.9	11.3	2.9	64.0	31.4	1.7	2.9
12% V_2O_5/SiO_2	2.6	13.3	2.8	62.2	32.8	3.0	2.0
1% V_2O_5/ZrO_2	2.0	38.8	98	51.0	19.0	30.0	
2% V_2O_5/ZrO_2	4.0	80.7	102	57.2	22.9	19.9	
4% V_2O_5/ZrO_2	8.1	145	92	58.5	18.0	23.5	

P_{C3} is the partial pressure of propane (moles per liter), and n represents the number of surface VO_4 species or catalytic active sites involved in the propane ODH rate-determining step (breaking of the C−H bond of the middle carbon in the propane molecule).[30] The zero-order dependence on the O_2 partial pressure and the first-order dependence on the propane partial pressure further reflect the almost fully oxidized state of the surface vanadia sites and the low surface coverage of reaction intermediates under the chosen reaction conditions, respectively. The value of n can be determined directly from the slope of the plot of log r vs log V as the surface vanadia coverage is varied in the submonolayer region, where the vanadia is 100% dispersed as surface vanadia species, at constant temperature and C_3 partial pressure. Such propane ODH kinetic plots are shown in Figure 9 for the supported vanadia catalysts and yield a slope of ∼1 for the different catalytic systems, which indicates that only one surface VO_4 site is involved in the rds for propane ODH to propylene.

4. Discussion

For dehydrated supported V_2O_5/SiO_2, the Raman band is constant at ∼1035 cm^{-1} at all surface vanadia coverage. For dehydrated supported V_2O_5/Al_2O_3 and V_2O_5/ZrO_2, the V═O vibration shifts with increasing surface vanadia coverage from 1018 to 1035 cm^{-1} and from 1027 to 1036 cm^{-1}, respectively. The corresponding UV−vis DRS measurements reveal that this shift to higher wavenumbers in the terminal V═O vibration parallels the extent of surface polymerization of the surface VO_4 on the Al_2O_3 and ZrO_2 supports. It appears that the dehydrated surface VO_4 species become more distorted, reflected in shorter V═O bond lengths and higher wavenumber values, as the surface vanadia transforms from isolated to polymeric species. Recently it has been proposed that the Raman vibration for the terminal V═O bond of the surface VO_4 on SiO_2 is vibrationally coupled to the silica support phonons at this frequency.[16] This may explain why the isolated surface VO_4 species vibrates at ∼1035 cm^{-1} when the same species on Al_2O_3 and ZrO_2 vibrate at 1018−1027 cm^{-1}; however, additional studies are required to fully understand such a vibrational coupling phenomenon.

The combined *in situ* Raman and UV−vis DRS studies on the same dehydrated supported vanadia catalysts also provide new insight into the nature of the ∼900 cm^{-1} Raman band typically observed for dehydrated supported metal oxide catalysts.[1−3,7,8,14−17,20,22,27,30−33,39] For the supported V_2O_5/Al_2O_3 catalytic system at low surface vanadia coverage (see Figure 2 and Table 1), UV−vis DRS reveals that only isolated surface VO_4 species are present at 0.3 V/nm^2 coverage and demonstrates that the corresponding broad Raman band in the ∼900 cm^{-1} region cannot originate from bridging V−O−V vibrations. For the supported V_2O_5/SiO_2 catalytic system (see Figure 1 and Table 1), Raman shows a band at ∼920 cm^{-1}; however, UV−vis DRS only shows the presence of isolated surface VO_4 species, which supports the conclusion that this vibration does not originate from bridging V−O−V vibrations. The same conclusion cannot be extended for the current supported V_2O_5/ZrO_2 catalytic system (see Figure 3 and Table 1) since polymeric surface vanadia species are present at all surface vanadia coverages in the samples examined, but the 930 cm^{-1} band is also clearly present at high surface coverage. The current experimental observations are in agreement with the recent theoretical DFT calculations of Magg et al.[16] that this vibration is not consistent with bridging V−O−V bonds, but originates

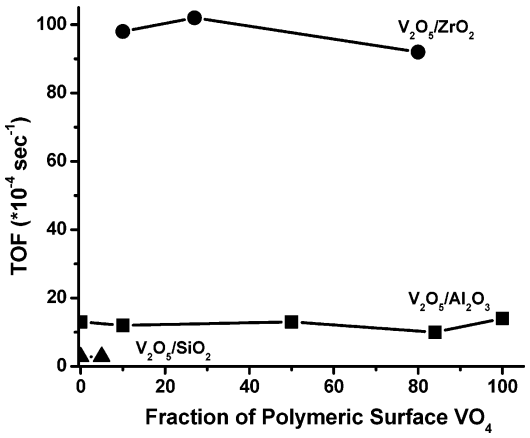

Figure 8. Propane ODH TOF as a function of fraction of polymeric surface VO_4 species for dehydrated supported V_2O_5/SiO_2, V_2O_5/Al_2O_3, and V_2O_5/ZrO_2 catalysts.

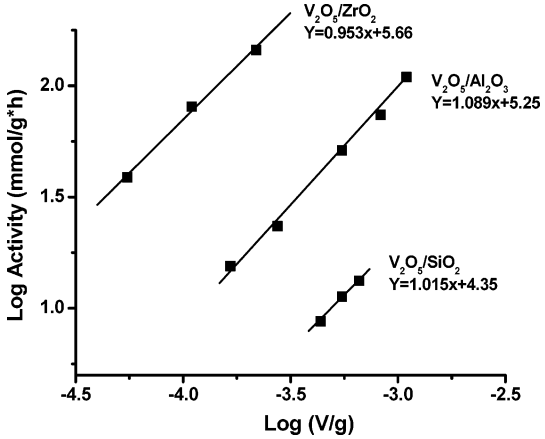

Figure 9. Plot of log[propane ODH catalytic activity (mmol/g·h)] vs log[*V*/g (V atoms/g)] loading with the slope corresponding to number of surface VO_4 sites involved in the kinetic rate determining step of propane activation.

from the bridging V−O−support bonds. Thus, Raman and IR bands typically observed at ~900 cm^{-1} for dehydrated supported surface metal oxide species[39] originate from the presence of bridging M−O−support bonds that anchor the surface metal oxide species to the underlying oxide support.

Although the Raman spectra of vanadia supported on other oxides are not reported here, the Raman spectra of all dehydrated supported vanadia catalysts exhibit a systematic increase in the wavenumber position of the terminal V═O bond of the surface VO_4 species with increasing surface vanadia coverage.[7,8,16,17,20,22,27,30−33] These Raman vibrational shifts are apparently also related to the increasing extent of polymerization of the surface VO_4 species with increasing surface vanadia coverage on these oxide supports. The same Raman vibrational shifts with increasing surface metal oxide coverage are also observed for most supported metal oxide catalyst systems (e.g., MoO_3, WO_3, CrO_3, Nb_2O_5, Ta_2O_5), suggesting that such Raman shifts are also related to polymerization of the dehydrated surface MO_x species with increasing surface metal oxide coverage.[17,39]

The UV−vis DRS E_g values for the dehydrated V_2O_5/SiO_2 catalysts are almost independent of surface vanadia coverage and exhibit values of 3.52−3.55 eV, which indicates that these samples exclusively contain isolated surface VO_4 species, confirming what is already known from other characterization studies.[4,12,16,18−22,34] For the dehydrated supported V_2O_5/Al_2O_3 catalysts, the E_g value continuously decreases with increasing surface vanadia coverage from 3.63 to 3.01 eV. The high E_g value at low surface vanadia coverage corresponds to 100% isolated surface VO_4 species and the lower E_g value at monolayer coverage corresponds to 100% polymeric surface VO_4 species, which is in agreement with the E_g values of the isolated VO_4 units present in bulk Na_3VO_4 (3.55 eV) and the polymeric VO_4 units present in bulk $NaVO_3$ (3.02 eV), respectively. The agreement in the E_g values between these bulk reference compounds and the dehydrated supported vanadia catalysts, as well as the absence of observed E_g values in the 2.3−2.8 eV range, further confirms that other surface vanadia species with greater than two bridging V−O−V bonds are either not present or are only present in a trace quantity. The continuous decrease in E_g values with increasing surface vanadia coverage on alumina reflects the increasing polymerization of the dehydrated surface VO_4 species as a function of surface coverage.[21] The same trend is observed for supported V_2O_5/ZrO_2 catalysts where the E_g value decreases from 3.50 eV at low surface coverage to 3.12 eV at monolayer coverage. The E_g values for the dehydrated supported V_2O_5/ZrO_2 indicate that isolated surface VO_4 species are the major species present at low surface vanadia coverage (~90% monomer) and become a minor species at monolayer coverage where the polymeric surface VO_4 species predominate (~80% polymer). With the exception of the supported V_2O_5/SiO_2 catalyst system, the dehydrated surface VO_4 species on oxide supports are essentially isolated monomers at low surface coverage (<2 V/nm^2) that progressively polymerize with increasing surface vanadia coverage and become extensively polymeric species at monolayer surface vanadia coverage (~8 V/nm^2). In addition, the specific oxide support cations also influence the extent of polymerization at a given surface coverage since at intermediate surface vanadia density the fraction of polymers on the supports is Al_2O_3 > ZrO_2 ≫ SiO_2.

The TOF values for propane ODH to propylene for each supported vanadia catalyst system were found to be almost invariant with surface vanadia coverage (extent of polymerization of the surface VO_4 species). This demonstrates that isolated surface VO_4 species and polymeric VO_4 species exhibit comparable catalytic activity for propane ODH to propylene and that the presence of bridging V−O−V bonds in the polymeric surface vanadia species does not affect the steady-state catalytic activity (see Figure 8). Simultaneously, the Raman vibration of the terminal V═O bond shifts for V_2O_5/Al_2O_3 (1018−1035 cm^{-1}) and V_2O_5/ZrO_2 (1027−1036 cm^{-1}) with increasing surface vanadia coverage arising from distortions caused by polymerization of the surface vanadia species. The invariance of the propane ODH reaction TOF value with these structural changes also suggests that the terminal V═O bond in the surface VO_4 species is not involved in the rate-determining step of the catalytic activation of the C−H bond of propane. This finding is consistent with the one VO_4 site requirement for the propane ODH reaction kinetics and suggests that an isolated surface VO_4 species catalytically functions similarly as an individual VO_4 unit that is part of a polymeric surface VO_4 chain structure. The propane ODH to propylene reaction is a two-electron process involving one O atom, reduction of V^{5+} to V^{3+}, which only requires one VO_4 unit. In summary, both isolated monomeric and polymeric surface VO_4 species catalytically function similarly during propane ODH and exhibit comparable TOF values on the same oxide support.

The constant propane ODH TOF values with surface vanadia coverage are somewhat surprising since many changes in the characteristics of the supported vanadia catalysts are simultaneously taking place with increasing surface coverage. As already discussed above, isolated surface vanadia species become progressively polymerized with increasing surface vanadia coverage. For the supported V_2O_5/Al_2O_3 catalyst system, both the surface Brønsted acidity and reducibility of the surface vanadia species are dependent on the surface vanadia coverage. Surface Brønsted acid sites begin to appear above ~2 V/nm^2, and their surface density rapidly increases with increasing surface coverage up to monolayer coverage.[41] Similarly, the reduction temperature for the surface vanadia species dramatically decreases, reflecting ease of reduction, above ~2 V/nm^2 with increasing surface vanadia coverage.[41] Although the polymerization of the surface VO_4 species significantly impacts both the surface Brønsted acidity and the reducibility of the surface vanadia species, it does not affect the propane ODH TOF value. Thus, the propane ODH reaction does not appear to be sensitive to either surface vanadia acidity or the surface vanadia redox properties.

The influence of the specific oxide support on the propane ODH TOF value of the surface VO_4 species is dramatic, as shown earlier in Table 2 and Figures 8 and 9. At low surface vanadia coverage, isolated surface VO_4 species are almost exclusively present for the supported 10% V_2O_5/SiO_2 (1.9 V/nm^2), 3% V_2O_5/Al_2O_3 (1.0 V/nm^2), and 1% V_2O_5/ZrO_2 (2.0 V/nm^2) catalysts. However, the corresponding TOF values for these catalysts vary by more than an order of magnitude with the specific oxide support: ZrO_2 > Al_2O_3 > SiO_2. This trend demonstrates that the specific catalytic activity of the isolated VO_4 species on the different oxide supports does not originate from a structural effect, monomer vs polymer, but arises from a ligand effect of the different support cations. At monolayer surface coverage (~8 V/nm^2), polymeric surface VO_4 units are the dominant surface vanadia species for V_2O_5/Al_2O_3 and V_2O_5/ZrO_2 and the propane TOF varies by a factor of ~5 for these two supported vanadia catalysts. The significant variation of the propane ODH TOF values for both isolated and polymerized surface VO_4 species with different supports demonstrates that the oxygen in the bridging V−O−support bond is the catalytic

active site involved in the kinetic rate determining step for propane activation over supported vanadia catalysts. Thus, the specific oxide support cation acts as a ligand that controls the catalytic activity of the bridging V−O−support bond for both isolated and polymerized surface VO_4 species.

The influence of the bridging V−O−support bond was also previously demonstrated by anchoring isolated surface VO_4 species on surface TiO_x, ZrO_x, and AlO_x monolayers on a SiO_2 support to form bilayered supported vanadia catalysts, where the underlying support cation was found to influence the TOF for methanol oxidation to HCHO by more than a factor of ~10.[41−44] This support effect was shown to be related to the electronegativity of the support cation in the bridging V−O−support bond. Decreasing the electronegativity of the support cation increases the basicity or electron density of the catalytic active oxygen in the bridging V−O−support bond and enhances its catalytic activity for redox reactions.[39]

For all supported metal oxide catalytic systems, the E_g values decrease with increasing surface MO_x coverage due to the increasing MO_x domain size (e.g., isolated surface MO_x species → polymeric surface MO_x → crystalline MO_x NPs) since the number of bridging M−O−M bonds generally increases with increasing domain size. The current propane ODH catalytic data show that, as the surface metal oxide domain size increases from isolated to polymeric species, the redox TOF values are essentially constant and independent of the decreasing E_g values. Consequently, the simultaneous increase in redox TOF values with decreasing E_g values sometimes reported for some catalytic systems may just be coincidental and related to other catalyst parameters being varied rather than related to the surface metal oxide domain size.

5. Conclusions

A quantitative method was developed to determine the surface concentrations of dehydrated monomeric and polymeric surface VO_4 species on SiO_2, Al_2O_3, and ZrO_2 supports. Supported V_2O_5/SiO_2 exclusively possesses isolated surface VO_4 species up to the maximum dispersion of the surface vanadia species (~2.6 V/nm^2). For supported V_2O_5/Al_2O_3 and V_2O_5/ZrO_2 catalysts, isolated surface VO_4 species are only present at low surface vanadia coverage and the extent of polymerization significantly increases with surface vanadia density up to monolayer surface coverage (~8 V/nm^2). This surface VO_4 polymerization trend as a function of surface vanadia coverage is also expected to take place on other oxide supports (e.g., TiO_2, Nb_2O_5, CeO_2).

The catalytic TOF for propane ODH to propylene, which only requires one surface VO_4 unit, is independent of the extent of polymerization of the surface VO_4 species, the E_g value, the surface Brønsted acidity, and the reducibility of the surface vanadia species, and is only a function of the specific oxide support. The oxide support cation acts as a potent ligand for the reactivity of surface VO_4 species by affecting the electron density or basicity of the bridging V−O−support bond, the catalytic active site involved in the kinetic rate determining step. The reactivity of the bridging V−O−support bonds is related to the support cation electronegativity, with low electronegativity increasing the basicity or electron density of the bridging V−O−support bond.

Acknowledgment. This research was financially supported by Department of Energy—Basic Energy Sciences Grant DEF-G02-93ER14350.

References and Notes

(1) Deo, G.; Wachs, I. E.; Haber, J. *Crit. Rev. Surf. Chem.* **1994**, *4*, 141.
(2) Wachs, I. E. Weckhuysen, B. M. *Appl. Catal., A* **1997**, *57*, 67.
(3) Weckhuysen, B. M.; Keller, D. E. *Catal. Today* **2003**, *78*, 25.
(4) Sun, Q.; Jehng, J. M.; Hu, H.; Herman, R. G.; Wachs, I. E.; Klier, K. *J. Catal.* **1997**, *165*, 91.
(5) Banares, M. A. *Catal. Today* **1999**, *51*, 379.
(6) Eon, J. G.; Olier, R.; Volta, J. C. *J. Catal.* **1994**, *209*, 318.
(7) Watling, T. C.; Deo, G.; Seshan, K.; Wachs, I. E.; Lercher, J. A. *Catal. Today* **1996**, *28*, 139.
(8) Khodakov, A.; Yang, J.; Su, S.; Igleasia, E.; Bell, A. T. *J. Catal.* **1998**, *177*, 343.
(9) Guliants, V. V. *Catal. Today* **1999**, *51*, 255.
(10) Al-Saeedi, J. N.; Guliants, V. V.; Guerrero-Perez, O.; Banares, M. A. *J. Catal.* **2003**, *215*, 108.
(11) Hazenkamp, M. F.; Blasse, G. *J. Phys. Chem.* **1992**, *96*, 3442.
(12) Das, N.; Eckert, H.; Hu, H.; Wachs, I. E.; Walzer J. F.; Feher, F. J. *J. Phys. Chem.* **1993**, *97*, 8240.
(13) Eckert, H.; Wachs, I. E. *J. Phys. Chem.* **1989**, *93*, 6796.
(14) Went, G. T.; Oyama, S. T.; Bell, A. T. *J. Phys Chem.* **1990**, *94*, 4240.
(15) Resini, C.; Montanari, T.; Busca, G.; Jehng, J.-M,; Wachs, I. E. *Catal. Today* **2005**, *99*, 105.
(16) Magg, N.; Immaraporn, B.; Giorgi, J. B.; Schroeder, T.; Baumer, M.; Dobler, J.; Wu, Z.; Kondratenko, E.; Cherian, M.; Baerns, M.; Stair, P. C.; Sauer, J.; Freund, H. *J. Catal.* **2004**, *226*, 88.
(17) Vuurman, M. A.; Wachs, I. E. *J. Phys. Chem.* **1992**, *96*, 5008.
(18) Yoshida, S.; Tanaka, T.; Hanada, T.; Hiraiwa, T.; Kanai, H.; Funabiki, T. *Catal Lett.* **1992**, *12*, 277.
(19) Gao, X.; Bare, S. R.; Weckhuysen, B. M.; Wachs, I. E. *J. Phys. Chem B* **1998**, *102*, 10842.
(20) Gao, X.; Banares, M. A.; Wachs, I. E. *J. Catal.* **1999**, *188*, 325.
(21) Gao, X.; Wachs, I. E. *J. Phys. Chem. B* **2000**, *104*, 1261.
(22) Gao, X.; Jehng, J.-M.; Wachs, I. E. *J. Catal.* **2002**, *209*, 43.
(23) Schraml-Marth, M.; Wokaun, A.; Pohl, M.; Kraus, H. L. *J. Chem. Soc., Faraday Trans.* **1991**, *87*, 2635.
(24) Catana, G.; Rao, R. R.; Weckhuysen, B. M.; Van Der Voort, P.; Vansant, E.; Schoonheydt, R. A.; *J. Phys. Chem. B* **1998**, *102*, 8005.
(25) Baltes, M.; Van Der Voort, P.; Vasant, E. F. *Langmuir* **1999**, *15*, 5841.
(26) Baltes, M.; Van Der Voort, P.; Weckhuysen, B. M.; Rao, R. R.; Catana, G.; Schoonheydt, R. A.; Vasant, E. F. *Phys. Chem. Chem. Phys.* **2000**, *2*, 2673.
(27) Argyle, M. D.; Chen, K.; Resini, C.; Krebs, C.; Bell, A. T.; Iglesia, E. *J. Phys. Chem. B* **2004**, *108*, 2345.
(28) Steinfeldt, N.; Muller, D.; Berndt, H. *Appl. Catal., A: Gen.* **2004**, *272*, 201.
(29) Knozinger, H.; Taglauer, E. *Catalysis* **1998**, *10*, 1.
(30) Chen, K.; Bell, A. T.; Iglesia, E. *J. Phys. Chem. B* **2000**, *104*, 1292.
(31) Olthof, B.; Khodakov, A.; Bell, A. T.; Iglesia, E. *J. Phys. Chem. B* **2000** *104*, 1516.
(32) Christodoulakis, A.; Machli, M.; Lemonidou, A.; Boghosian, S. *J. Catal.* **2004**, *222*, 293.
(33) Zhao, Z.; Gao, X., Wachs, I. E. *J. Phys. Chem. B* **2003**, *107*, 6333.
(34) Xie, S.; Bell, A. T.; Iglesia, E. *Langmuir* **2000**, *16*, 7162.
(35) Tian, H.; Wachs, I. E. To be published.
(36) Ross, E. I.; Wachs, I. E. To be published.
(37) Barker, M. G.; Hoper, A. J. *J. Chem. Soc., Dalton Trans.* **1973**, *15*, 1513.
(38) Charles, N.; Caughlan, N.; Smith, H. M.; Watenpaigh, K. *Inorg. Chem.* **1966**, *12*, 2131.
(39) Wachs, I. E. *Catal. Today* **1996**, *27*, 437; *Catal. Today* **2005**, *100*, 79.
(40) Turek, A. M.; Wachs, I. E.; Decanio, E. *J. Phys. Chem.* **1992**, *96*, 5000.
(41) Gao, X.; Wachs, I. E. *J. Catal.* **2000**, *192*, 18.
(42) Gao, X.; Fierro, J. L. G.; Wachs, I. E. *Langmuir* **1999**, *15*, 3169.
(43) Gao, X.; Bare, S. R.; Fierro, J. L. G.; Wachs, I. E. *J. Phys. Chem. B* **1999**, *103*, 618.
(44) Gao, X.; Wachs, I. E. *Top. Catal.* **2000**, *11/12*, 85.